J Therm Anal Calorim (2011) 106:267–275
DOI 10.1007/s10973-011-1726-z

Thermal behaviour of nickel(II) sulphate, nitrate and halide complexes containing ammine and ethylenediamine as ligands

Kinetics and evolved gas analysis

K. S. Rejitha · Suresh Mathew

NATAS2010 Conference Special Issue

Abstract Thermal behaviour of nickel amine complexes containing SO_4^{2-}, NO_3^-, Cl^- and Br^- as counter ions and ammonia and ethylenediamine as ligands have been investigated using simultaneous TG/DTA coupled with mass spectroscopy (TG/DTA–MS). Evolved gas analyses detected various transient intermediates during thermal decomposition. The nickel ammonium sulphate complex produces NH, N, S, O and N_2 species. The nickel ammonium nitrate complex generated fragments like N, N_2, NO, O_2, N_2O, NH_2 and NH. The halide complexes produce NH_2, NH, N_2 and H_2 species during decomposition. The ligand ethylenediamine is fragmented as N_2/C_2H_4, NH_3 and H_2. The residue hexaamminenickel(II) sulphate produces NiO with crystallite size 50 nm. Hexaammine and tris(ethylenediamine)nickel(II) nitrate produce NiO in the range 25.5 nm and 23 nm, respectively. The halide complexes produce nano sized metallic nickel (20 nm) as the residue. Among the complexes studied, the nitrate containing complexes undergo simultaneous oxidation and reduction.

Keywords Kinetic parameters · Nickel amine complexes · Non-mechanistic equations · Thermal behaviour

Introduction

The thermal decomposition studies of transition metal amine complexes have generated great interests among thermal analysis community [1, 2]. During heating, these complexes undergo stepwise decomposition to form various intermediates. In air, most of the complexes give metal oxide as the final residue [3]. However, in inert atmosphere, metal is obtained as the final product [2]. In this study, we have investigated in detail the thermal decomposition behaviour of certain nickel amine complexes containing ammonia and ethylenediamine as the ligands viz., hexaamminenickel(II) and tris(ethylenediamine)nickel(II) sulphate, hexaammine-nickel(II) and tris(ethylenediamine)nickel(II) nitrate and hexaamminenickel(II) halides (chloride and bromide). We have detected the evolved gaseous species during the thermal decomposition of these amine complexes using TG–MS. Evolved gas analysis (EGA) offers a useful tool to identify the species formed during thermal decomposition [4, 5].

Kinetic parameters determined for different stages of thermal decomposition of these amine complexes were evaluated using four non-mechanistic equations viz., Coats–Redfern (CR), Madusudanan–Krishnan–Ninan (MKN), Horowitz–Metzger (HM) and MacCallum–Tanner (MT) [6–9].

Experimental

The nickel complexes were synthesized as per the procedure reported in the literature [10]. Nickel content in the complexes was determined by gravimetry [11]. The complexes were further characterized by spectral and chemical analysis. The halide content in the complexes was determined by Volhard's method [11].

Instrumentations

TG/DTA–MS studies were carried out using a Rigaku TG-8120 instrument combined with mass spectroscopy

K. S. Rejitha · S. Mathew (✉)
School of Chemical Sciences, Mahatma Gandhi University, P.D. Hills, Kottayam 686 560, Kerala, India
e-mail: sureshmathews@sancharnet.in

(Anelva, M-QA200TS) under high-purity He gas flow (99.9999%). The heating rate employed was 10 °C min^{-1}. Samples were loaded in a platinum crucible, and the mass was kept constant around 10 ± 0.1 mg.

X-ray powder patterns were recorded on a Bruker D8 Advance diffractometer (using Cu Kα radiation, $\lambda = 1.542$ Å).

Mathematical treatment of data

Non-mechanistic equations

The non-mechanistic equations are given below

The Coats–Redfern equation

$$\ln\frac{g(\alpha)}{T^2} = \ln\left[\frac{AR}{\phi E}\left(1-\frac{2RT}{E}\right)\right] - \frac{E}{RT} \quad (1)$$

The MKN equation

$$\ln\left[\frac{g(\alpha)}{T^{1.9215}}\right] = \ln\frac{AE}{\phi R} + 3.7721 - 1.9215\ln E - \frac{0.12039E}{T} \quad (2)$$

The Horowitz–Metzger equation

$$\ln g(\alpha) = \ln\frac{ARTs^2}{\phi E} - \frac{E}{RTs} + \frac{E\theta}{RTs^2} \quad (3)$$

The MacCallum–Tanner equation

$$\log_{10} g(\alpha) = \log_{10}\frac{AE}{\phi R}0.483E^{0.435} - \frac{(0.449+0.217E)10^3}{T} \quad (4)$$

where, $g(\alpha) = \frac{1-(1-\alpha)^n}{1-n}$, n is the order parameter, and α is the extent of decomposition. T_s is the DTG peak temperature, and θ is $(T - T_s)$.

The order parameter n was determined using the Coats–Redfern equation by an iteration method. Linear plots of $\ln[g(\alpha)/T^2]$ against $1/T$ were plotted by least square method, taking α and T values from the TG curve. Linear curves were drawn for different values of n ranging from 0 to 2 in increment of 0.01. The value of n is selected by the best fit having maximum correlation coefficient.

Plotting L. H. S. of Eqs. 1, 2, 4 against $1/T$ and (3) against θ, gives straight line. From the slope and the intercept, E and A can be calculated.

The entropy of activation was calculated using the following equation

$$A = \left(\frac{kT_s}{h}\right)\exp\left(\frac{\Delta S^{\#}}{R}\right) \quad (5)$$

where k is the Boltzmann constant, h is the Planck's constant and $\Delta S^{\#}$ is the entropy of activation.

Results and discussion

Thermal decomposition studies

Sulphate complexes

TG/DTA–MS patterns for hexaamminenickel(II) sulphate and tris(ethylenediamine)nickel(II) sulphate are shown in Fig. 1a, b, respectively and their themoanalytical data are

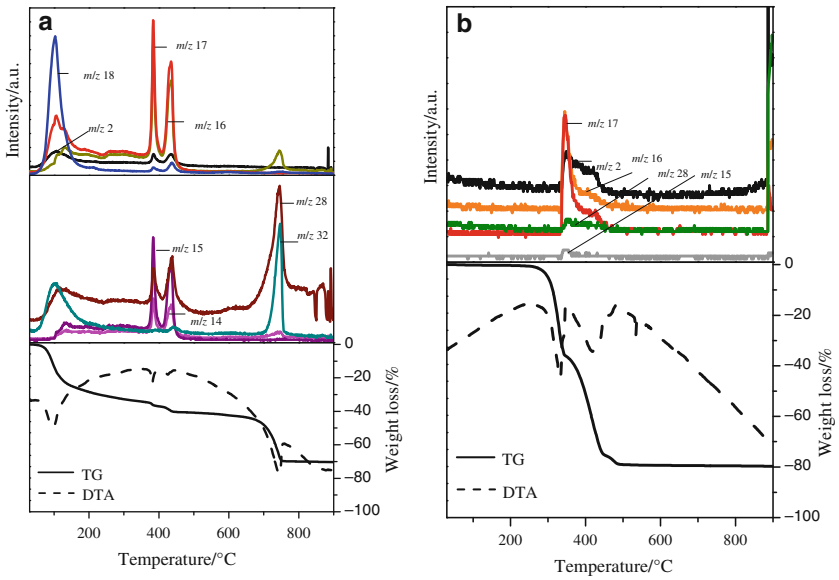

Fig. 1 **a** TG/DTA–MS plot of hexaamminenickel(II) sulphate and **b** tris(ethylenediamine)-nickel(II) sulphate at heating rate 10 °C min^{-1})

Table 1 Thermo analytical data for the decomposition of complexes/$\Phi = 10$ °C min^{-1}

Complexes	Stages	TG results			Percentage weight loss		Residue	Fragments evolved
		T_i/°C	T_f/°C	T_s/°C	Theoretical	Observed		
$[Ni(NH_3)_6]SO_4$	I	89.8	184.8	139.9	26.5	26.5	$Ni(NH_3)_2SO_4$	SO_3, NH, N, N_2, S, O_2 and O
	II	186	310.5	297	6.7	6.5	$Ni(NH_3)SO_4$	
	III	312	487	452.9	6.7	6.5	$NiSO_4$	
	IV	634	845	804	31.2	31.2	NiO	
$[Ni(en)_3]SO_4$	I	270	380	346	35.8	36	$Ni(en)SO_4$	H_2, NH, NH_2, NH_3 N_2 and CH_2=CH_2
	II	380	520	480	–	–	Mixture of Ni_3S_2 and Ni	
$[Ni(NH_3)_6](NO_3)_2$	I	78	116	87	5.97	5.7	$Ni(NH_3)_5(NO_3)_2$	H_2O, NH, NH_2, N, O, N_2, NO, O_2 and N_2O
	II	116	164	136	5.97	5.8	$Ni(NH_3)_4(NO_3)_2$	
	III	164	300	266	61.9	61.3	NiO	
$[Ni(en)_3](NO_3)_2$	I	220	300	262	79.4	78	NiO	H_2O, H_2, N, NH_2, NH_3, N_2, C_2H_4, NO and N_2O
$[Ni(NH_3)_6]Cl_2$	I	79	140	132	29.3	28.9	$Ni(NH_3)_2Cl_2$	H_2, N, NH, NH_2 and N_2
	II	140	280	250.7	14.7	14.3	$NiCl_2$	
	III	609	743.8	727.8	30.6	31.8	Ni	
$[Ni(NH_3)_6]B_2$	I	90	180	155.5	21.2	21	$Ni(NH_3)_2B_2$	H_2, NH, NH_2 and N_2
	II	180	260	239.6	10.6	10	$NiBr_2$	
	III	580.5	726.7	716.8	49.9	49	Ni	

Table 2 Thermal decomposition stages of complexes

Complexes	Stages	Decomposition
$[Ni(NH_3)_6]SO_4$	I	$[Ni(NH_3)_6]SO_4 \rightarrow Ni(NH_3)_2SO_4 + 4NH_3$
	II	$Ni(NH_3)_2SO_4 \rightarrow Ni(NH_3)SO_4 + NH_3$
	III	$Ni(NH_3)SO_4 \rightarrow NiSO_4 + NH_3$
	IV	$NiSO_4 \rightarrow NiO + SO_3$
$[Ni(en)_3]SO_4$	I	$[Ni(en)_3]SO_4 \rightarrow Ni(en)SO_4 + 2en$
	II	$4Ni(en)SO_4 \rightarrow Ni_3S_2 + Ni + 4en + 8O_2 + 2S$
$[Ni(NH_3)_6](NO_3)_2$	I	$[Ni(NH_3)_6](NO_3)_2 \rightarrow Ni(NH_3)_5(NO_3)_2 + NH_3$
	II	$Ni(NH_3)_5(NO_3)_2 \rightarrow Ni(NH_3)_4(NO_3)_2 + NH_3$
	III	$Ni(NH_3)_4(NO_3)_2 \rightarrow NiO + 4NH_3 + NO_3 + NO_2$
$[Ni(en)_3](NO_3)_2$	I	$[Ni(en)_3](NO_3)_2$ NiO + gaseous products
$[Ni(NH_3)_6]Cl_2$	I	$[Ni(NH_3)_6]Cl_2 \rightarrow Ni(NH_3)_2Cl_2 + 4NH_3$
	II	$Ni(NH_3)_2Cl_2 \rightarrow NiCl_2 + 2NH_3$
	III	$NiCl_2 \rightarrow Ni + Cl_2$
$[Ni(NH_3)_6]Br_2$	I	$[Ni(NH_3)_6]Br_2 \rightarrow Ni(NH_3)_2Br_2 + 4NH_3$
	II	$Ni(NH_3)_2Br_2 \rightarrow NiBr_2 + 2NH_3$
	III	$NiBr_2 \rightarrow Ni + Br_2$

given in Table 1. Hexaamminenickel(II) sulphate having a four stage thermal decomposition is given in Table 2.

For the hexaamminenickel(II) sulphate complex, the decomposition starts at 75 °C and ends at 220 °C. The weight loss (26.5%) indicates that this decomposition is associated with the liberation of four molecules of ammonia. The temperatures of inception (T_i) for the second and third stages are 330 and 390 °C, respectively. The final temperature (T_f) values of these two stages are 390 and 440 °C, respectively. For both these stages, the weight loss observed (6.2 and 6.1%) correspond to the loss of one molecule of ammonia each to give anhydrous nickel sulphate. Nickel sulphate is stable up to 650 °C and then starts to decompose. This step has a weight loss of 31.2%

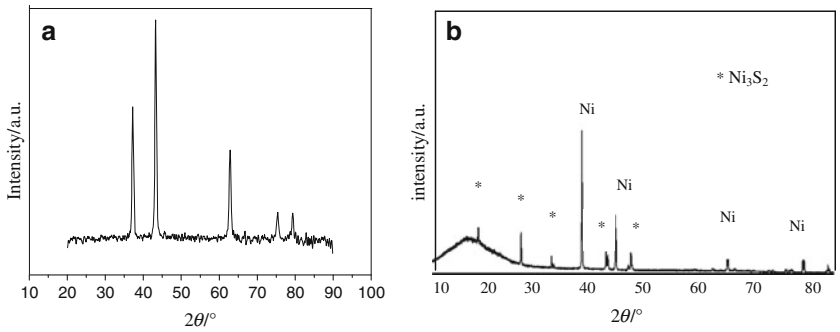

Fig. 2 **a** XRD pattern of NiO and **b** mixture of nickel and Ni_3S_2

corresponding to the decomposition of nickel sulphate, eventually leading to the formation of nickel oxide as the final residue. Figure 2a shows the XRD pattern of NiO.

The observed thermal decomposition pattern is in agreement with the single crystal data of the complex. The complex has a distorted octahedral symmetry [12]. The six ammonia ligands are crystallographically different. The four ammonia molecules lying in the square planar plane experience some strain due to the distortion which results from the complicated hydrogen bonding between the SO_4^{2-} tetrahedra and the different ammine ligands of the $[Ni(NH_3)_6]^{2+}$ octahedra [12, 13]. This may lead to the easier removal of four ammonia ligands during heating. Thereafter, the complex adopts a linear structure with two ammonia molecules having Ni–N bond distances 213.1 and 212.5 pm and N–Ni–N bond angle 179.6°. On heating, the ammonia molecule which occupies at a distance 213.1 pm is expected to get evolved first followed by the other ammonia molecule.

In the MS plot, ion peak with *m*/*z* value 18 corresponds to the adsorbed moisture in the complex. Peaks with *m*/*z* value 17 at 103.3, 389 and 433.8 °C correspond to the evolved ammonia, which is in accordance with the thermal decomposition of the complex. Ion peaks with *m*/*z* values 2 and 16 can be attributed to the presence of H_2 and NH_2, respectively. In the mass spectra some other peaks with *m*/*z* values 15, 14 and 28 are also seen. These peaks correspond to NH, N and N_2, respectively, and these species can also be formed from ammonia. During the final stage of decomposition, SO_3 (80) is evolved and is fragmented into various species as shown in Scheme 1.

The plot of simultaneous TG/DTA coupled online with MS pattern of tris(ethylenediamine)nickel(II) sulphate indicates (Fig. 1b) two stage thermal decomposition pattern. The final product of the decomposition is a mixture of

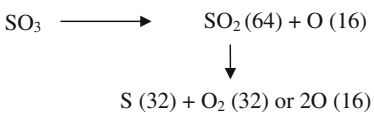

Scheme 1 Fragmentation of sulphur trioxide

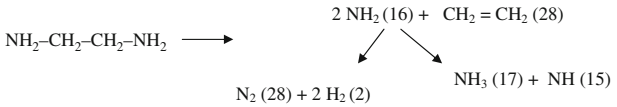

Scheme 2 Fragmentation of ethylenediamine

metallic nickel and Ni_3S_2 confirmed by X-ray diffractometry (Fig. 2b).

For this complex, the decomposition starts at 270°Cand ends at 380 °C with the loss of two molecules of ethylendiamine. The second stage begins at 380 °C and ends at 520 °C with the formation of a mixture of Ni_3S_2 and Ni phases as the residue.

The mass spectra of tris(ethylenediamine)nickel(II) sulphate show peaks with *m*/*z* values 2, 15, 16, 17 and 28. These peaks are due to the presence of H_2, NH, NH_2, NH_3 and N_2/CH_2=CH_2. These species are formed due to the fragmentation of the liberated molecule as shown in Scheme 2.

Nitrate complexes

Simultaneous TG/DTA coupled with mass spectral plot of hexaamminenickel(II) nitrate and tris(ethylenediamine)nickel(II) sulphate are shown in Fig. 3a, b and their phenomenological details are given in Table 1.

The hexaammine complex starts to lose mass at 78 °C with the liberation of one molecule of ammonia. The second stage at 116 °C is also a deamination stage in which one molecule of ammonia is liberated to give an intermediate tetraammine complex. Third stage involves (164–300 °C) the simultaneous deamination and decomposition of the tetraammine complex to give NiO as the final residue. The formation of NiO is confirmed by XRD analysis and is given in Fig. 4a.

TG–MS plot reveals the presence of ion peak with mass number 17 in the temperature range 78–164 °C, indicating the evolution of ammonia. Along with the peaks of ammonia, ion peaks with mass numbers 15 and 16 were also observed during this temperature range. This could be due to the presence of NH and NH_2 ion species. The peaks corresponding to *m*/*z* values 14, 16, 28, 30, 32 and 44 indicate the presence of ions like N, O, N_2, NO, O_2 and

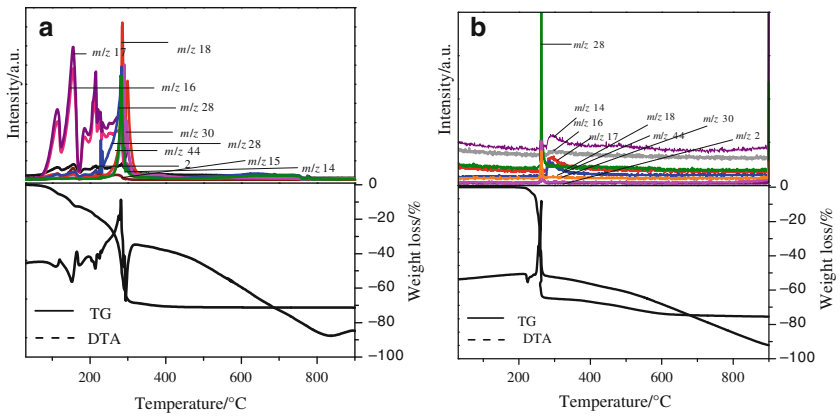

Fig. 3 **a** TG/DTA–MS plot of hexaamminenickel(II) nitrate and **b** tris(ethylenediamine) nickel(II) nitrate at heating rate 10 °C min^{-1}

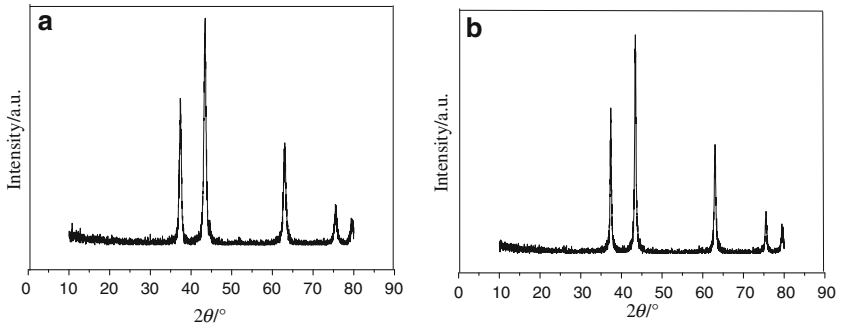

Fig. 4 XRD patterns of NiO formed from **a** hexaamminenickel(II) nitrate **b** tris(ethylenediamine)nickel(II) nitrate

N_2O formed by the fragmentation of NO_3 group. The possible fragmentation pattern for NO_3 is shown in Scheme 3.

The oxidation of ammonia also generates gaseous species like NO and N_2O. The presence of ion peak with *m/z* value 18 can be attributed to the formation of water. The formation and evolution of water has been reported during the thermal decomposition of $Co(NH_3)_6(NO_3)_2$, $Pd(NH_3)_2(NO_2)_2$ and $Pt(NH_3)_2(NO_2)_2$ complexes [14, 15]. The formation of water due to the reaction between the evolved gaseous products is shown in Scheme 4 [15].

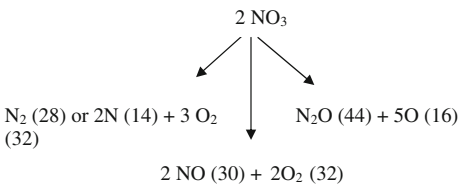

Scheme 3 Fragmentation of NO_3

$$2\,NH_3 + 3\,O_2 + N_2 \rightarrow 2\,NO + N_2O + 3\,H_2O$$
$$\text{or } 2\,NH_3 + 2.5\,O_2 \rightarrow 2\,NO + 3\,H_2O$$

Scheme 4 Formation of water from gaseous products

The TG/DTA–MS profile of tris(ethylenediamine)-nickel(II) nitrate (Fig. 3b), shows that this complex decomposes at 220 °C in a single step to give nickel oxide as the residue (Fig. 4b).

The gaseous products include the oxides of nitrogen and ethylenediamine. It is seen from the mass spectra that the possible gaseous products like NO_3 and NO_2 are fragmented to different species like N, O, N_2, NO and N_2O ion species. The fragmentation possibility of ethylenediamine and nitrate group is shown in Schemes 2 and 3, respectively.

In the mass spectra (Fig. 3b), the ion peaks with mass numbers 2, 14, 16, 17, 18, 28, 30 and 44 were observed during the thermal decomposition of this complex. These peaks appear in the temperature range 260–290 °C and correspond to the formation of ion species like H_2, N, NH_2, NH_3, H_2O, N_2/C_2H_4, NO and N_2O. The detection of oxides of nitrogen formed from the fragmentation of NO_3^- group in the temperature range 260–290 °C, surmise the presence of $Ni(NO_3)_2$ phase during the thermal decomposition of the tris(ethylenediamine) complex. Among the ion peaks, H_2, N, NH_3 and N_2 are formed by in situ fragmentation of the evolved ethylenediamine as shown in Scheme 2.

Mass numbers 16, 30 and 44 correspond to the presence of O, NO and N_2O formed by the fragmentation of NO_3^- group as shown in Scheme 3. Detection of water (*m/z* 18) possibly formed by the reaction between the gaseous

products (Scheme 4) was also observed in the mass spectral analysis of tris(ethylenediamine) complex.

Halide complexes

The plot of simultaneous TG/DTA coupled online with MS for $[Ni(NH_3)_6]Cl_2$ and $[Ni(NH_3)_6]Br_2$ are given in Fig. 5a, b. The phenomenological data and the thermal decomposition pattern for hexaamminenickel(II) halides are given in Table 1 and Table 2 respectively.

The first stage of thermal decomposition of hexaamminenickel(II) chloride is in the temperature range 79–140 °C, and this stage corresponds to the release of four ammonia molecules. Broadly, the second stage of decomposition comprises the release of two ammonia molecules in the temperature range 140–280 °C. (However, a very slow mass loss is observed in the TG depicting the partial release of ammonia in the temperature regime 140–200 °C. A close perusal of the DTA curve shows a small endothermic (T_P = 185 °C) peak indicating this slight mass loss of 2%). This second stage of deamination corresponds to the release of two ammonia molecules resulting in the formation of $NiCl_2$ (mass loss 14.3%). The decomposition of $NiCl_2$ commences at 609 °C and the mass loss of 31.8%, corresponding to the release of chlorine resulting in the formation of metallic nickel at 744 °C as the residue. The XRD pattern of the metallic nickel is shown in Fig. 6a.

Mass spectra recorded during the thermal decomposition of hexaamminenickel(II) chloride show a strong peak with *m/z* value 17, signaturing the release of four ammonia molecules at 132 °C as the first deamination. The MS peak (*m/z* 17) with very low intensity at 184 °C and an intense ion peak (*m/z* 17) at 266 °C substantiate the TG results. TG–MS analysis shows ion peaks with mass numbers 2, 14, 15, 16 and 28. These mass numbers indicate the presence of ion fragments like H_2, N, NH, NH_2 and N_2, respectively. The evolution of Cl_2 or its fragments during the final stage of thermal decomposition is not detected in the TG–MS.

Hexaamminenickel(II) bromide complex has a three stage thermal decomposition pattern (Fig. 5b). The thermal decomposition of hexaamminenickel(II) bromide starts at 90 °C with the loss of four molecules of ammonia. The

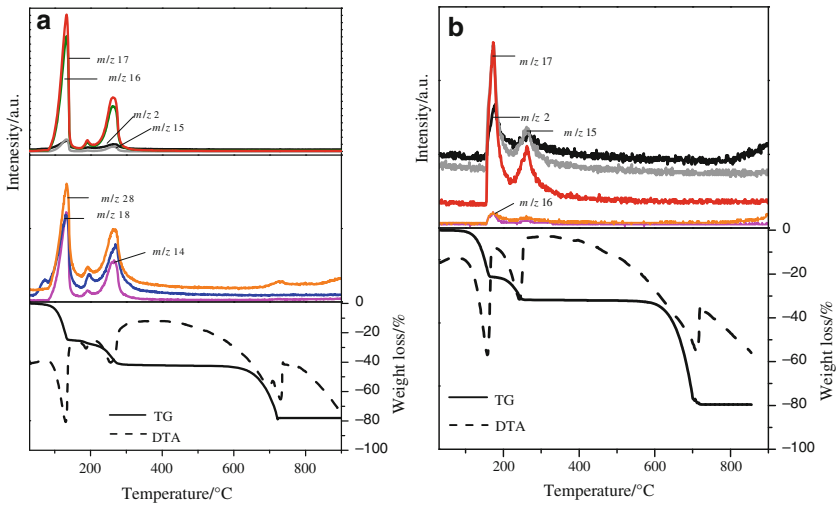

Fig. 5 **a** TG/DTA–MS plot of hexaamminenickel(II) chloride and **b** hexaamminenickel(II) bromide at heating rate 10 °C min^{-1}

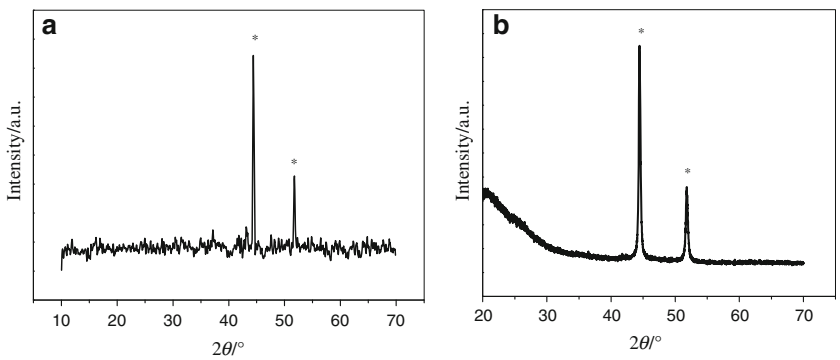

Fig. 6 XRD patterns of Ni formed from **a** hexaamminenickel(II) chloride **b** hexaamminenickel(II) bromide

second stage of deamination involves the liberation of two ammonia molecules in the temperature range 180–260 °C. The third decomposition stage begins at 580.5 °C and corresponds to the release of bromine. The mass loss of 49% at this stage corresponds to the formation of metallic nickel as the residue (Fig. 6b) as evident by the X-ray analysis.

The MS ion peak at 165 °C with *m*/*z* 17 corresponds to the first deamination stage (release of four ammonia molecules) in the TG. Ion peak with mass number 17 at 250 °C indicates the evolution of two ammonia molecules. The observed intensity of the two MS peaks are consistent with the amount of ammonia released viz., four molecules of ammonia in the first stage and two molecules of ammonia in the second stage of thermal decomposition. MS analysis has also detected peaks with *m*/*z* values 2, 15, 16 and 28. These peaks are due to H_2 NH, NH_2 and N_2 fragments formed by the decomposition of ammonia as shown below.

$$5NH_3(17) \rightarrow NH(15) + 2NH_2(16) + N_2(28) + 5H_2(2)$$

The liberation of Br_2 or its fragments, during the final stage of decomposition is not detected by the mass spectral analysis.

Kinetic studies

The kinetic parameters for the thermal decomposition reactions of the complexes were evaluated from the TG curves using the four non-mechanistic equations viz., Coats–Redfern, Madhusudanan–Krishnan–Ninan, Horowitz–Metzger and MacCallum–Tanner, and the values are shown in Tables 3, 4, 5, 6, 7.

The kinetic parameters obtained for the various stages of thermal decomposition of hexaamminenickel(II) sulphate are shown in Table 3. From Table 3, it is seen that the correlation coefficients (*r*) are in the range 0.9927–0.9994, indicating nearly perfect fits. The activation energy is the highest for the fourth stage of decomposition. Same trend is shown by the pre-exponential factor and the entropy of the activation for stage IV and it can be due to the kinetic compensation effect. The first stage of deamination is having the next highest value of activation energy. The values for kinetic parameters obtained for second and third stages of deamination are lower. The kinetic parameters obtained using the four non-mechanistic equations are almost same. However, the values of KP obtained for Horowitz–Metzger equation are comparatively high, and it is due to the discrepancy involved in the approximation employed in the Horowitz–Metzger equation.

It can be seen that the order parameters are decimal value. It is known from the literature [16] that the order parameters can have a decimal number. The entropy of activation has negative values. The negative values indicate that the activated complex has an ordered structure than the reactant, and the reaction in this case is said to be slower than the normal [17].

Table 3 Kinetic parameters for the thermal decomposition stages of hexaamminenickel(II) sulphate using non-mechanistic equations

	Stage I	Stage II	Stage III	Stage IV
n	1.25	0.6	1.48	0.47
E/kJ mol^{-1}				
CR	84.6	42.3	43.1	311.8
MKN	84.7	42.7	43.4	312.2
HM	90.7	60.7	61.2	320.9
MT	84.5	42.4	43.3	315.1
A/s^{-1}				
CR	3.8×10^8	2.5×10^1	4.1×10^0	7.6×10^{12}
MKN	4.3×10^8	3.0×10^1	5.2×10^0	8.4×10^{12}
HM	2.2×10^9	1.8×10^3	1.2×10^1	6.8×10^{14}
MT	3.9×10^8	2.7×10^1	3.9×10^0	8.6×10^{13}
$\Delta S^{\#}$/JK^{-1} mol^{-1}				
CR	-8.3×10^1	-2.2×10^2	-2.4×10^2	-8.2×10^0
MKN	-8.2×10^1	-2.2×10^2	-2.4×10^2	-8.9×10^0
HM	-6.8×10^1	-1.9×10^1	-2.1×10^2	-2.8×10^0
MT	-8.1×10^1	-2.2×10^1	-2.3×10^1	-2.2×10^0
r				
CR	0.9993	0.9929	0.9944	0.9992
MKN	0.9993	0.9929	0.9945	0.9992
HM	0.9978	0.9927	0.9958	0.9991
MT	0.9994	0.9953	0.9946	0.9993

Table 4 Kinetic parameters for the first deamination reaction of tris(ethylenediamine)nickel(II) sulphate using non-mechanistic equations ($n = 0.74$)

Equations	*E*/kJ mol^{-1}	*A*/s^{-1}	$\Delta S^{\#}$/JK^{-1} mol^{-1}	*r*
CR	254.4	2.2×10^{19}	1.2×10^2	0.9974
MKN	247.9	6.1×10^{18}	1.1×10^2	0.9975
HM	258.9	5.0×10^{19}	1.3×10^2	0.9963
MT	253.1	2.1×10^{19}	1×10^2	0.9977

The kinetic parameters viz., *E*, *A* along with the values of correlation coefficients obtained for the first deamination stage of tris(ethylenediaminenickel)(II) sulphate is shown in Table 4.

The values of kinetic parameters obtained from different non-mechanistic equations are comparable. The entropy is found to have a positive value. The decomposition stage with positive entropy indicates that the activated complex has a less-ordered structure and the reaction in this case is said to be faster than the normal [17]. It can be seen from the table that the order parameter for the decomposition process is decimal numbers

Table 5 Kinetic parameters for the two deamination stages of hexaamminenickel(II) nitrate decomposition from non-mechanistic equations

	Stage I	Stage II
n	1.47	1.49
E/kJ mol^{-1}		
CR	125.80	101.37
MKN	125.82	100.65
HM	161.25	105.46
MT	124.60	99.62
A/(s^{-1})		
CR	1.23×10^{14}	5.95×10^{10}
MKN	1.34×10^{14}	5.01×10^{10}
HM	2.83×10^{20}	1.83×10^{11}
MT	8.23×10^{16}	3.40×10^{10}
$\Delta S^{\#}$/JK^{-1} mol^{-1}		
CR	-2.34×10^{1}	-4.14×10^{1}
MKN	-1.61×10^{1}	-4.28×10^{1}
HM	-1.44×10^{2}	-3.21×10^{1}
MT	-7.65×10^{1}	-4.61×10^{1}
r		
CR	0.9982	0.9976
MKN	0.9982	0.9976
HM	0.9982	0.9964
MT	0.9984	0.9979

Table 6 Kinetic parameters for the first deamination and dechlorination of hexaamminenickel(II) chloride from non-mechanistic equations

	Stage I	Stage III
n	0.37	1.1
E/kJ mol^{-1}		
CR	76.2	248.8
MKN	76.4	248.9
HM	92	260.1
MT	76.1	248.7
CR	1.1×10^{7}	1.9×10^{22}
A/s^{-1}		
MKN	1.2×10^{7}	2.0×10^{22}
HM	1.1×10^{9}	2.4×10^{23}
MT	1.0×10^{7}	1.9×10^{22}
CR	-1.1×10^{2}	1.8×10^{2}
$\Delta S^{\#}$/JK^{-1} mol^{-1}		
MKN	-1.1×10^{2}	2.0×10^{2}
HM	-7.5×10^{1}	2.4×10^{2}
MT	-1.1×10^{2}	1.8×10^{2}
CR	0.9997	0.9952
r		
MKN	0.9997	0.9952
HM	0.9992	0.995
MT	0.9992	0.9955

The first two clear cut and non overlapping deamination reactions of hexaamminenickel(II) nitrate involving the loss of one ammonia molecule in each stage are subjected to kinetic analysis. The kinetic parameters obtained are given in Table 5.

Kinetic parameters computed from the four non-mechanistic equations are comparable. The values of correlation coefficient in the table show good linear fit. It can be seen from the table that the order parameters are fractional numbers. It is known from the literature [16] that the order parameters can have decimal number. The entropy of the activation for the two deamination stages shows negative values. The negative values of entropy indicate that the activated complex has an ordered structure than the reactant, and the reaction in this case is said to be slower than the normal [17]. The kinetic parameters (E and A) calculated for the first deamination stage (i.e. hexaamminenickel(II) nitrate to pentaamminenickel(II) nitrate) show higher values compared with the second stage of deamination (pentaamminenickel(II) nitrate to tetraamminenickel(II) nitrate). This can be due to the stable crystal structure of hexaamminenickel(II) nitrate.

In the case of hexaamminenickel(II) chloride complex, the first deamination reaction involving the loss of four

Table 7 Kinetic parameters for the thermal decomposition of hexaamminenickel(II) bromide from non-mechanistic equations

	Stage I	Stage II	Stage III
n	0.54	0.2	1.48
E/kJ mol^{-1}			
CR	70.4	71.2	273.1
MKN	70.6	69.9	272.7
HM	84.3	85.9	304.7
MT	70.3	71.1	271.1
A/s^{-1}			
CR	5.1×10^{6}	3.9×10^{4}	2.9×10^{14}
MKN	5.8×10^{6}	2.9×10^{4}	2.9×10^{14}
HM	3.3×10^{8}	1.2×10^{6}	2.5×10^{16}
MT	4.9×10^{6}	3.2×10^{4}	2.7×10^{14}
$\Delta S^{\neq}$/JK^{-1} mol^{-1}			
CR	-1.2×10^{2}	-1.6×10^{2}	2.3×10^{1}
MKN	-1.2×10^{2}	-1.6×10^{2}	2.3×10^{1}
HM	-8.5×10^{1}	-1.3×10^{2}	6.0×10^{1}
MT	-1.2×10^{2}	-1.4×10^{2}	2.2×10^{1}
r			
CR	0.9998	0.9949	0.9932
MKN	0.9998	0.9946	0.9932
HM	0.9991	0.9955	0.9929
MT	0.9998	0.9959	0.9931

ammonia molecules and the dechlorination reaction were subjected to kinetic analysis since these stages involve clear cut and non overlapping reactions. The kinetic parameters evaluated from the non-mechanistic equations for hexaamminenickel(II) chloride are given in Table 6.

It is observed that the kinetic parameters obtained for hexaamminenickel(II) chloride from the four non-mechanistic equations are comparable. The correlation coefficients obtained are 0.9950–0.9997, indicating perfect fits. The highest activation energy is obtained for the dechlorination reaction, probably due to the stable nickel chloride structure. The apparent order parameters obtained are decimal values. The deamination reaction (hexaamminenickel(II) chloride → diamminenickel(II) chloride) of the complex has negative entropy values, which indicate that for these processes the activated complex has a more-ordered structure than the reactant, and the reactions are described as slower than the normal. The dechlorination reaction shows positive entropy values, which indicate that for these processes the activated complex has a less-ordered structure, and the reactions are said to be slower than the normal [17].

The kinetic parameters computed for hexaamminenickel(II) bromide complex, from the four non-mechanistic equations are given in Table 7, and the obtained values are comparable.

The correlation coefficients obtained are in the range 0.9931–0.9998, indicating perfect fits. For hexaamminenickel(II) bromide complex, debromination reaction (stage III) possesses the highest activation energy, probably due to the stable nickel bromide structure. The two deamination reactions (stage I and II) of the complex have negative entropy values, which indicate that for these processes the activated complex has a more-ordered structure than the reactant, and the reactions are described as slower than the normal. The debromination reaction shows positive entropy values, which indicate that for these processes the activated complex has a less-ordered structure, and the reactions are said to be slower than the normal [17].

Conclusions

A comparative study on the thermal decomposition behaviour of some nickel amine complexes were carried out by means of simultaneous TG/DTA coupled with mass spectroscopy (TG/DTA–MS). Nickel complexes containing SO_4^{2-}, NO_3^-, Cl^- and Br^- as counter ions and ammonia and ethylenediamine as ligands have been employed for the investigation. The decomposition products from the complexes were identified by in situ evolved gas analyses. The final decomposition products of the complexes were identified by means of X-ray diffraction studies. The decomposition kinetics of the complexes was calculated using non-mechanistic equations.

Acknowledgements The authors are grateful to Prof. T. Ichikawa, the Institute for Advanced Materials Research, Hiroshima University, Japan, for the TG–MS analyses.

References

1. Mathew S, Nair CGR, Ninan KN. Thermal decomposition kinetics: kinetics and mechanism of thermal decomposition of tetraamminecopper(II) sulphate monohydrate. Thermochim Acta. 1989;144:33–43.
2. Kapoor IPS, Kapoor M, Singh G, Singh UP, Goel N. Preparation, characterization and thermolysis of nitrate and perchlorate salts of 2,4,6-trimethylaniline. J Hazard Mater. 2010;173:173–80.
3. Mathew S, Nair CGR, Ninan KN. Thermal decomposition kinetics: kinetics and mechanism of thermal decomposition of bis(ethylenediamine)copper(II) halide monohydrate. Thermochim Acta. 1991;181:253–8.
4. Alcolea A, Ibarra I, Caparrós A, Rodríguez R. Study of the MS response by TG–MS in an acid mine drainage efflorescence. J Therm Anal Calorim. 2010;101:1161–5.
5. Yu Z, Sun Y, Wei W, Lu L, Wang X. Preparation of $NdCrO_3$ nanoparticles and their catalytic activity in the thermal decomposition of ammonium perchlorate by DSC/TG-MS. J Therm Anal Calorim. 2009;97:903–9.
6. Coats AW, Redfern JP. Kinetic parameters from thermogravimetric data. Nature. 1964;201:68–9.
7. Madhusudanan PM, Krishnan K, Ninan KN. A new approximation for the p(x) function in the evaluation of non-isothermal kinetic data. Thermochim Acta. 1986;97:189–201.
8. Horowitz HH, Metzger G. A new analysis of thermogravimetric traces. Anal Chem. 1963;35:1464–8.
9. MacCallum JR, Tanner J. The kinetics of thermogravimetry. Eur Polym J. 1970;6:1033–9.
10. Rochow EG, editor. Inorganic synthesis, vol. 6. New York: McGraw-Hill; 1960.
11. Vogel AI. A text book of quantitative inorganic analysis. 4th ed. New York: Longmann; 1978.
12. Mockenhaupt C, Eßmann R, Lutz HD. $[Ni(NH_3)_6]SO_4$: crystal structure and infra red spectra. Z Naturforsch. 1999;54b:843–8.
13. Cotton FA, Wilkinson G. Advanced inorganic chemistry. 5th ed. New York: Wiley; 1988.
14. Skoczylas ML, Mikuli E, Szklarzewicz J, Hetmańczyk J. Thermal behaviour, phase transition and molecular motions in $[Co(NH_3)_6](NO_3)_2$. Thermochim Acta. 2009;496:38–44.
15. Madarász J, Bombicz P, Mátyás C, Réti F, Kiss G, Pokol G. Comparative evolved gas analytical and structural study on trans-diammine-bis(nitrito)-palladium(II) and platinum(II) by TG/DTA-MS, TG-FTIR, and single crystal X-ray diffraction. Thermochim Acta. 2009;490:51–9.
16. Norris AC, Pope MI, Selwood M. The determination of kinetic parameters for reactions involving solids. Thermochim Acta. 1980;41:357–60.
17. Frost AA, Pearson RG. Kinetics and mechanism. New York: Wiley; 1961.